

Electrooxidation of Methanol on AuNi/C Catalyst in Alkaline Medium

Liquan Lu^{1,*}, Shichao Zhang², Shaohui Yan³

¹ School of Mechatronics Engineering, North University of China, Taiyuan 030051, China

² School of Materials Science and Engineering, Beihang University, Beijing 100191, China

³ College of Environmental Science and Engineering, Taiyuan University of Technology, Taiyuan, 030024, China

*E-mail: lq_lu@buaa.edu.cn

Received: 10 October 2014 / Accepted: 19 November 2014 / Published: 2 December 2014

AuNi/C catalyst (AuNi nanoparticles supported on activated carbon) is prepared by a polyol reduction process. The alloying between Au and Ni and the removal of unalloyed Ni are achieved by the heat and acid treatment. The electrochemical measurement results indicate that the alloying treatment process is favourable to improve the electrocatalytic activity of the AuNi/C catalyst. Moreover, the area-specific electrochemical activity of each AuNi/C catalyst is better than that of the Au/C catalyst, showing the effect of the Ni component on the electrocatalytic activity of the Au/C catalyst is significant.

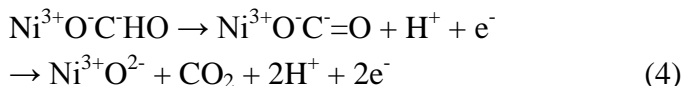
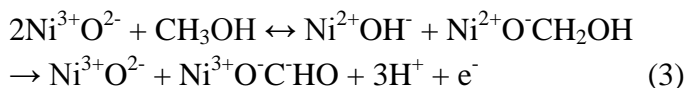
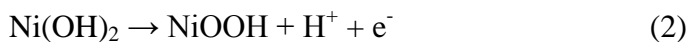
Keywords: Direct methanol fuel cells; Electrocatalyst; AuNi/C; Electrooxidation; Alloying

1. INTRODUCTION

The anodic reaction of direct methanol fuel cell (the methanol electrooxidation, MEO) involves the transfer of six electrons to the electrode for complete oxidation to carbon dioxide [1,2]. At present, Pt catalyst with the best activity for the MEO is still one of main research objects [3-6]. However, the strong adsorption of the CO-like intermediates (CO_{ads}) yielded from the MEO on the surface of the Pt catalyst results in its activity growing gradually weaker [6-9]. To bypass this impediment, great efforts have been made by researchers. The most common approach to promote the CO tolerance of the Pt catalyst is to alloy Pt with oxophilic elements, such as Ru, Ni, Fe, Sn, Co, Pd, Zn, Ag ect. [3-7,9-14]. The enhanced catalytic property can be accounted for by the bifunctional mechanism and the electronic (ligand) effect mechanism [6,7,9,12,15]. According to the bifunctional mechanism, the methanol is oxidized on the Pt sites to form the CO_{ads} , while the dissociative adsorption of H_2O is occurred on the

surface of the oxophilic element to yield the activated oxygen species (OH_{ads}) [6,9,15,16]. The CO_{ads} can be easily electrooxidized by the neighboring OH_{ads} to form the CO_2 , which releases the Pt active sites [6,9,15,16]. The main idea of the electronic effect mechanism is that the addition of the oxophilic element changes the electronic state of the Pt, which influences the activation of the methanol C-H bond or Pt-adsorbate binding [12,15].

More recently, it has been reported that the addition of the Ni component in the Pt catalyst can significantly improve its electro-catalytic activity and CO tolerance [17-24]. Therefore, the research related to the improvement of the Ni component to the Pt catalyst has been a focus of intensive research in recent years. Fu et al. synthesized the Pt-rich shell coated Ni nanoparticles with high electro-catalytic activity and good CO tolerance [17]. The electrooxidation of methanol in sulfuric acid solution was investigated on the Pt, Pt/Ni, Pt/Ru/Ni, and Pt/Ru alloy nanoparticle catalysts synthesized using a conventional reduction method [20]. The research results indicate that the catalytic activities of the Pt/Ni and Pt/Ru/Ni alloy catalysts are better than those of the pure Pt and Pt/Ru catalysts. The improvement of the Ni component on the Pt and Pt/Ru catalysts can be interpreted by the following reaction schemes [20]:



Based on the bifunctional mechanism and the improvement of the Ni component on the electrochemical activity of the Pt catalyst, we investigated the MEO on the AuNi/C catalyst synthesized by impregnation method in ethyleneglycol system [25]. The research results reveal that the AuNi/C catalyst annealed at 400 °C exhibits excellent electrochemical activity and stability for the MEO. Moreover, the similar results are obtained by investigating the MEO on the AuFe/C catalyst; that is to say, the AuFe/C catalyst treated at 400 °C shows high electrochemical activity for the MEO [26]. Analogously, other carbon supported Au-based alloy catalysts annealed at 400 °C should also display good catalytic activity for the MEO. Therefore, we prepare the AuNi/C alloy nanoparticle catalyst by a glycol process, and investigate the effect of the heat treatment temperature on its catalytic activity for the MEO.

2. EXPERIMENTAL

2.1. Synthesis of the AuNi/C catalysts

The typical procedure for the preparation of the AuNi/C catalyst is as follows: firstly, 12 ml 0.024 M HAuCl_4 and 1.15 ml 0.5 M NiCl_2 aqueous solutions are mixed in a boiling flask-3-neck. Secondly, 172 mg of activated carbon is dispersed in the above mixed solution using ultrasonic agitation for 30 min. Then, the mixed solution in the boiling flask-3-neck is vigorously stirred using an

electric mixer. In the agitating process, 6 folds NaOH aqueous solution (6.9 ml, 1.0 M) is rapidly added into the boiling flask-3-neck. 10 minutes later, 20 ml ethylene glycol is added in the mixed solution. Afterwards, it is heated on a heating apparatus. When the temperature reaches to the constant boiling point (about 140 °C) of the mixed solution, it becomes boiling. When the temperature of the mixed solution is increase again, stop heating the mixture, because the water in the mixed solution is boiled away [27]. After the mixed solution cooling to the home temperature, it is moved into a 35 ml reaction kettle. Thereafter, the fill factor is adjusted to approximately 80% by adding ethylene glycol. Whereafter, the reaction kettle is heated using an oven at 200 °C for 5 h. After aging for 12 h, the as-prepared AuNi/C composition is diluted with 20 ml ethanol, collected through filtering, washed adequately with ethanol and dried in a vacuum drying oven at 60 °C for 5 h. Subsequently, the AuNi/C composition is respectively annealed at 300, 400, 500 and 600 °C in nitrogen atmosphere for 2 h to alloy the Au and Ni components. Then, the annealed catalysts are soaked in 0.5 M H₂SO₄ solution for 12 h to remove the unalloyed Ni. Finally, the AuNi/C catalysts are filtered, fully washed and dried in a vacuum drying oven at 60 °C for 5 h. The AuNi/C catalysts treated at different temperatures are denoted as AuNi/C_x, where x is the heat treatment temperature.

2.2. Characterization of the AuNi/C catalysts

The morphology of the AuNi/C catalysts is investigated using a JEM 2100F transmission electron microscope (TEM, JEOL). The X-ray powder diffraction (XRD) data of the AuNi/C catalysts are collected using a D/max 2200PC (Rigaku) X-ray diffractometer with a graphite monochromator and Cu *Kα*1 radiation ($\lambda = 0.15406$ nm) at a step rate of 0.02 ° s⁻¹. The components of the AuNi/C catalysts are determined by an Oxford INCA energy dispersive X-ray spectroscopy (EDS) equipped on an S-530 Scanning Electron Microscope (SEM, HITACHI).

2.3. Electrochemical studies

The cyclic voltammograms (CVs) on the AuNi/C catalysts are recorded in the deoxygenated 0.5 M H₂SO₄ solution using a CHI660D electrochemical workstation (Shanghai, China) at the ambient temperature (~ 25 °C), to calculate their electrochemically active surface areas (ECSA) with the amounts of electricity involved in the reduction of the Au oxide monolayer, according to a value of 386 $\mu\text{C cm}^{-2}$ Au [28,29]. The electrocatalytic activities of the AuNi/C catalysts for the MEO are investigated using cyclic voltammetry in the deaerated 0.1 M KOH with 5 M CH₃OH solution. The scan rate is 20 mV s⁻¹. The working electrode is fabricated according to the method described in literature [25,30-32]. Briefly, 5 μL catalyst ink, prepared by mixing 2.0 mg AuNi/C catalyst, 950 μL ethanol and 50 μL Nafion solution (5 wt%, DuPont Corp., USA), is placed on a polished glassy carbon working electrode ($\Phi = 4$ mm) using a microsyringe. A saturated calomel electrode (SCE) and a mercury|mercury oxide electrode (Hg|HgO, 1.0 M KOH) are respectively employed as the reference electrodes in H₂SO₄ and KOH media. A sheet of glassy carbon (0.9 cm²) is used as the counter

electrode. Prior to electrochemical measurements, the electrolytes are deaerated by bubbling with high-purity nitrogen for 30 min.

3. RESULTS AND DISCUSSION

3.1. The effect of the heat treatment on the morphology of the AuNi/C catalysts

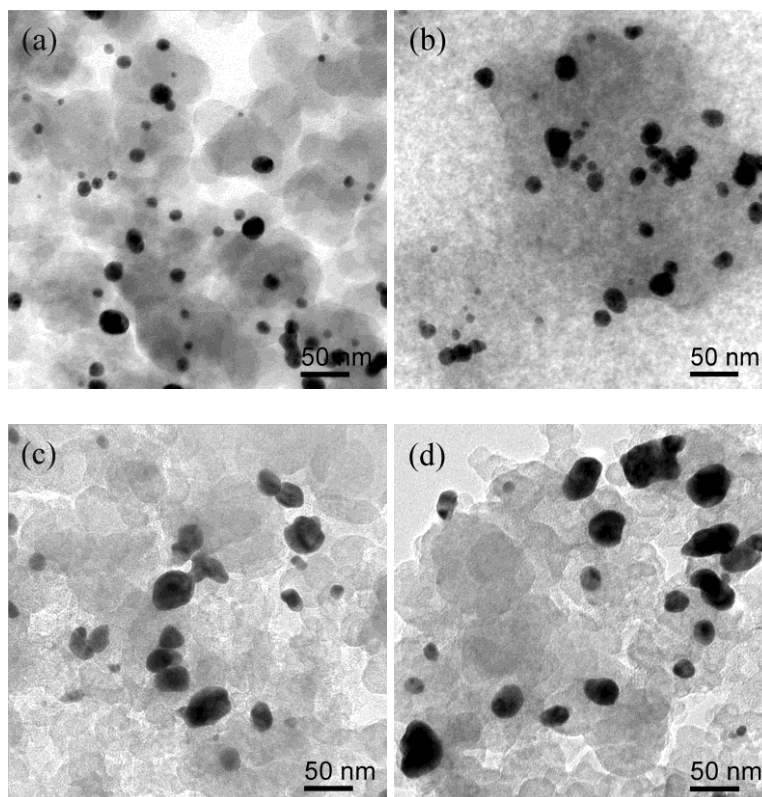


Figure 1. TEM images of the AuNi/C300 (a), AuNi/C400 (b), AuNi/C500 (c) and AuNi/C600 (d) catalysts.

The TEM images of the AuNi/C catalysts annealed at different temperatures are shown in Fig. 1, which indicates the average sizes of the AuNi nanoparticles in these catalysts increase with the rise in the heat treatment temperature. According to Fig. 1, it is found that, the mean size of the AuNi nanoparticles is increased significantly, only when the heat treatment temperature is higher than 400 °C. Furthermore, the amount of the AuNi nanoparticles with small size gradually diminishes as the heat treatment temperature rises, implying that abundant AuNi nanoparticles with small size are consumed, during the formation of the AuNi nanoparticles with large size.

3.2. The effect of the heat treatment on the components of the AuNi/C catalysts

The EDS spectra of the AuNi/C catalysts are shown in Fig. 4. The Au loadings of the AuNi/C300, AuNi/C400, AuNi/C500 and AuNi/C600 catalysts determined by the EDS analysis are

29.77%, 29.41%, 29.64% and 29.71%, respectively. The chemical compositions of the AuNi nanoparticles and the components of the AuNi/C catalysts analysed by EDS are listed in Table 1. According to the chemical compositions and Ni loadings of the AuNi nanoparticles listed in Table 1, the Ni contents of the AuNi nanoparticles in the AuNi/C catalysts first increase and then decrease as the heat treatment temperature rises, and the Ni content of the AuNi/C400 catalyst is the highest. The changing trend of the Ni content in the AuNi/C catalyst with the increase in the heat treatment temperature is similar to the previous research [25]. This is related to the AuNi system phase-separate in the AuNi nanoparticle [25].

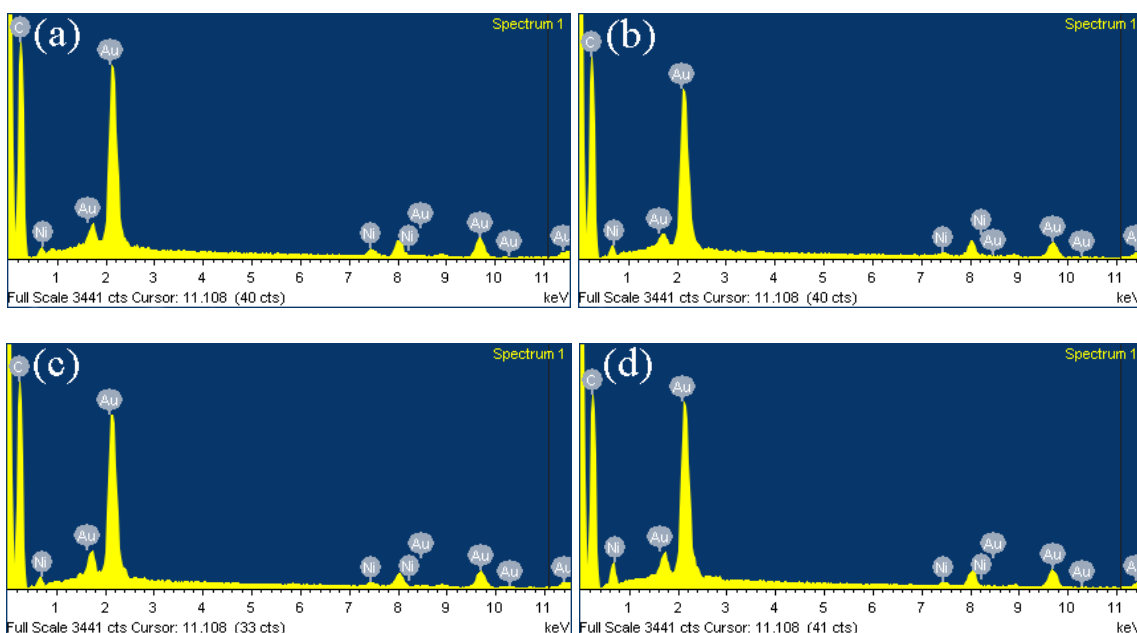


Figure 2. EDS spectra of the AuNi/C300 (a), AuNi/C400 (b), AuNi/C500 (c) and AuNi/C600 (d) catalysts.

Table 1. The components of the AuNi/C catalysts determined by EDS and the chemical compositions of the AuNi nanoparticles.

catalyst	weight percent			atomic percent			chemical composition
	m _C %	m _{Au} %	m _{Ni} %	n _C %	n _{Au} %	n _{Ni} %	
AuNi/C300	69.46	29.77	0.77	97.24	2.54	0.22	Au ₉₂ Ni ₈
AuNi/C400	68.61	29.41	1.98	96.9	2.53	0.58	Au ₈₁ Ni ₁₉
AuNi/C500	69.15	29.64	1.21	97.12	2.53	0.35	Au ₈₈ Ni ₁₂
AuNi/C600	69.31	29.71	0.98	97.17	2.54	0.29	Au ₉₀ Ni ₁₀

3.2. The effect of the heat treatment on the structure of the AuNi/C catalysts

The XRD patterns of the AuNi/C catalysts are given in Fig. 3, in which the species of the AuNi/C catalysts are displayed. As can be observed from Fig. 3, the characteristic diffraction peaks of the AuNi/C300 respectively locate at around $2\theta = 38.3, 44.5, 64.7$ and 77.6° , which correspond to the

(111), (200), (220) and (311) lattice planes of the face-centered cubic (fcc) structure of gold, respectively. This phenomenon suggests that the crystal lattice parameters of the AuNi/C300 hardly change as a result of the addition of the Ni component. It is interesting to note from Fig.3 that the diffraction peaks corresponding to the (311) lattice plane denoted by red and blue lines first shift to higher and then to lower 2θ values with the enhancement of the heat treatment temperature. Moreover, the diffraction peak of the AuNi/C400 has the highest 2θ value. Surprisingly, there is a positive correlation between the positions of the diffraction peaks corresponding to the AuNi nanoparticles in the AuNi/C catalyst and its Ni loading. That is, the diffraction peaks of the AuNi nanoparticles in the AuNi/C catalyst shift to higher 2θ values with the increase in the Ni loading of the AuNi/C catalyst. This implies that the structure of the AuNi nanoparticles in the AuNi/C catalyst is the Au fcc structure with negligible distortion. According to the previous research, the AuNi alloy phase should be the Au based AuNi alloy phase [25,33]. For the materials with the fcc structure, the relations between the crystal lattice constant and the angle of the (220) diffraction peak meet the following equation [34]:

$$\alpha_{fcc} = \frac{\sqrt{2} \cdot \lambda_{K\alpha 1}}{\sin \theta_{(220)}} \quad (5)$$

where, α_{fcc} is the crystal lattice constant of the materials with the fcc structure, $\theta_{(220)}$ is the angle of the (220) diffraction peak and $\lambda_{K\alpha 1}$ is the X-ray wavelength (1.54056 Å for Cu $K\alpha 1$ radiation). On the basis of Eq. 5 and Fig. 3, the crystal lattice constant of AuNi alloy phase is smaller than that of Au phase.

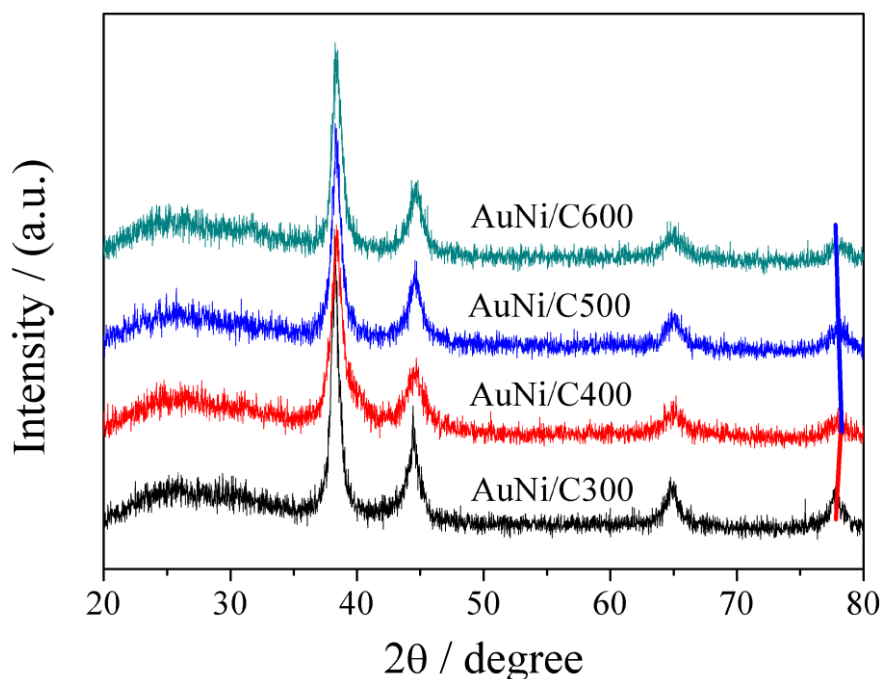


Figure 3. XRD patterns of the AuNi/C300 (a), AuNi/C400 (b), AuNi/C500 (c) and AuNi/C600 (d) catalysts.

Moreover, the crystal lattice constant of the AuNi alloy nanoparticles in the AuNi/C catalyst first increase and then decrease with the increase in the heat treatment temperature. This suggests that

the alloying degree of the AuNi nanoparticles with the Au based AuNi alloy phase and its Ni loading are directly related.

3.4. The methanol electrooxidation on the AuNi/C catalyst

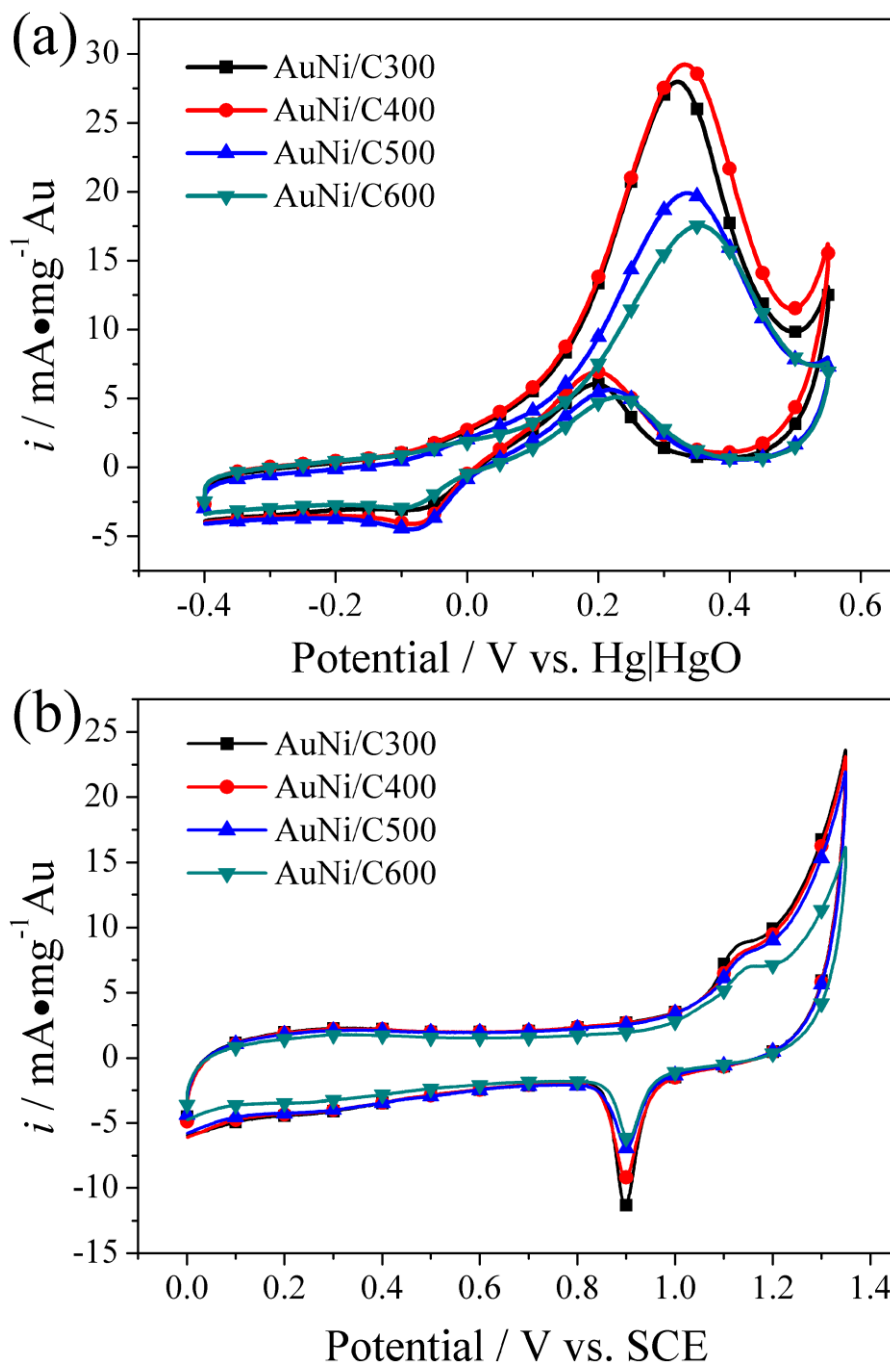


Figure 4. CVs on the AuNi/C catalysts at a scan rate of 20 mV s^{-1} in the deoxygenated $0.1 \text{ M KOH} + 5 \text{ M CH}_3\text{OH}$ (a) and $0.05 \text{ M H}_2\text{SO}_4$ (b) solutions. The species of the AuNi/C catalysts are shown in the figures.

Fig. 4a is the CVs on the AuNi/C catalysts at a scan rate of 20 mV s^{-1} in the deoxygenated $0.1 \text{ M KOH} + 5 \text{ M CH}_3\text{OH}$ mixed solution. The current densities in the Fig. 4 are normalized by the Au loadings listed in Table 1. Fig. 4a reveals that the maximum mass-specific current densities of the AuNi/C300, AuNi/C400, AuNi/C500 and AuNi/C600 catalysts for the MEO are 27.98、29.26、19.88 and $17.57 \text{ mA mg}^{-1} \text{ Au}$, respectively. For further studying the catalytic activities of the AuNi/C catalysts for the MEO, their electrochemically active surface areas (ECSA) are calculated using the amounts of electricity involved in the reduction of the Au oxide monolayer, according to a value of $386 \mu\text{C cm}^{-2} \text{ Au}$ [28,29]. The CVs on the AuNi/C catalysts in $0.05 \text{ M H}_2\text{SO}_4$ solution are shown in Fig. 4b. The estimated ECSA of the AuNi/C300, AuNi/C400, AuNi/C500 and AuNi/C-600 are 69.4、61.3、43.3 and $37 \text{ cm}^2 \text{ mg}^{-1} \text{ Au}$, respectively. Therefore, the peak values of the ECSA current densities for the AuNi/C300, AuNi/C400, AuNi/C500 and AuNi/C600 catalysts are 0.4、0.48、0.46 and $0.47 \text{ mA cm}^{-2} \text{ Au}$, respectively. Compared to the AuNi/C300 catalyst, the AuNi/C400, AuNi/C500 and AuNi/C600 catalysts have higher ECSA activities for the MEO, showing the increase in the alloying degree of the AuNi nanoparticles (i. e. the enhancement of the Ni loading in the AuNi nanoparticles) is helpful for the improvement of the ECSA activity of the AuNi/C catalyst. When the atomic percent of the Ni component in the AuNi nanoparticles is more than 10%, however, its maximum ECSA current density hardly increases with the enhancement of the alloying degree. When the heat treat temperature is higher than $400 \text{ }^\circ\text{C}$, moreover, the mean diameters of the AuNi nanoparticles in the AuNi/C catalyst increase dramatically, resulting to its ECSA decrease significantly. This reduces the mass-specific activity of the AuNi/C catalyst. Therefore, the AuNi/C400 catalyst reveals the highest mass-specific current density, due to its small AuNi nanoparticles and proper alloying degree. The effect laws of the heat treatment temperature on the ECSA activity and mass-specific activity of the AuNi/C catalyst synthesized by the glycol process is similar to the previous investigation [25]. Compared to the Au/C-20% catalyst (around $0.38 \text{ mA cm}^{-2} \text{ Au}$) reported in previous literature [35], the ECSA activities of the AuNi/C catalysts are all improved. The reason for the increase in the electrocatalytic activity of the AuNi/C catalyst can be explain using the bifunctional mechanism. The NiOOH formed at a low electrode potential according to Eqs. 1 and 2 has excellent auxiliary catalysis to the electrooxidation of the methanol molecule adsorbed on the adjacent Au site [25]. Combining with our previous research [25,26], all the carbon supported Au based catalysts annealed at $400 \text{ }^\circ\text{C}$ reveal excellent electrocatalytic activities. The main reason is the Au based nanoparticles in the AuNi/C catalysts treated at this temperature have the minor diameter and proper alloying degree. For the carbon supported Au based catalyst prepared by one-step method, therefore, $400 \text{ }^\circ\text{C}$ is a suitable heat treatment temperature.

4. CONCLUSIONS

The AuNi/C catalyst is successfully synthesized by the glycol process, and the impact of the heat treatment temperature on its activity for the MEO is investigated using cyclic voltammetry. The research results indicate the Ni contents of the AuNi nanoparticles in the as-prepared AuNi/C catalysts first increase and then decrease as the heat treatment temperature rises, and the alloying degree of the

AuNi nanoparticles with the Au based AuNi alloy phase and its Ni loading have notable positive correlation. Although the enhancement of the alloying degree between the Au and Ni components is favorable to improve the ECSA activity of the AuNi/C catalyst, its ECSA activity hardly enhances when the atomic percent of the Ni component in the AuNi nanoparticles are more than 10%. When the heat treat temperature is higher than 400 °C, however, the mean diameters of the AuNi nanoparticles in the AuNi/C catalyst increase dramatically. Therefore, the AuNi nanoparticles in the AuNi/C400 catalyst remain the minor diameter and proper alloying degree, causing that it reveals the highest mass-specific activity. Combining with our previous research, we propose that 400 °C is a suitable heat treatment temperature to improve the electrocatalytic activity of the carbon supported Au based catalyst synthesized by one-step method.

ACKNOWLEDGEMENTS

This work is supported by the Natural Science Foundation of Shanxi (2014011017-2), Scientific and Technological Innovation Programs of Higher Education Institutions in Shanxi (STIP, 2014113), National Basic Research Program of China (2013CB934001) and Natural Science Foundation of Beijing (2051001).

References

1. A. S. Aricò, S. Srinivasan, V. Antonucci, *Fuel Cells*, 1 (2001) 133.
2. L. Carrette, K. A. Friedrich, U. Stimming, *Fuel Cells*, 1 (2001) 5.
3. F. Alcaide, G. Álvarez, P. L. Cabot, H. J. Grande, O. Miguel, A. Querejeta, *Int. J. Hydrogen Energy*, 36 (2011) 4432.
4. S. S. Mahapatra, A. Dutta, J. Datta, *Int. J. Hydrogen Energy*, 36 (2011) 14873.
5. M. Khorasani-Motlagh, M. Noroozifar, M. S. Ekrami-Kakhki, *Int. J. Hydrogen Energy*, 36 (2011), 11554.
6. K. Koczkur, Q. Yi, A. Chen, *Adv. Mater.*, 19 (2007) 2648.
7. F. Liu, Q. Yan, W. J. Zhou, X. S. Zhao, J. Y. Lee, *Chem. Mater.*, 18 (2006) 4328.
8. R. Awasthi, R. N. Singh, *Int. J. Hydrogen Energy*, 37 (2012) 2103.
9. F. Liu, J. Y. Lee, W. Zhou, *Adv. Funct. Mater.*, 15 (2005) 1459.
10. A. Galal, N. F. Atta, H. K. Hassan, *Int. J. Electrochem. Sci.*, 7 (2012) 768.
11. S. H. Ahn, O. J. Kwon, S. K. Kim, I. Choi, J. J. Kim, *Int. J. Hydrogen Energy*, 35 (2010) 13309.
12. H. Yang, J. Zhang, K. Sun, S. Zou, J. Fang, *Angew. Chem. Int. Ed.*, 49 (2010) 6848.
13. C. T. Hsieh, W. M. Hung, W. Y. Chen, J. Y. Lin, *Int. J. Hydrogen Energy*, 36 (2011) 2765.
14. H. Wang, S. Ji, W. Wang, V. Linkov, S. Pasupathi, R. Wang, *Int. J. Electrochem. Sci.*, 7 (2012) 3390.
15. R. Liu, H. Iddir, Q. Fan, G. Hou, A. Bo, K. L. Ley, E. S. Smotkin, Y. E. Sung, H. Kim, S. Thomas, A. Wieckowski, *J. Phys. Chem. B*, 104 (2000) 3518.
16. E. Ticanelli, J. G. Beery, M. T. Paffett, S. Gottesfeld, *J. Electroanal. Chem.*, 258 (1989) 61.
17. X. Z. Fu, Y. Liang, S. P. Chen, J. D. Lin, D. W. Liao, *Catal. Commun.*, 10 (2009) 1893.
18. J. Mathiyarasu, A. M. Remona, A. Mani, K. L. N. Phani, V. Yegnaraman, *J. Solid State Electr.*, 8 (2004) 968.
19. F. Ye, S. Chen, X. Dong, W. Lin, *J. Nat. Gas Chem.*, 16 (2007) 162.
20. K. W. Park, J. H. Choi, B. K. Kwon, S. A. Lee, Y. E. Sung, H. Y. Ha, S. A. Hong, H. Kim, A. Wieckowski, *J. Phys. Chem. B*, 106 (2002) 1869.

21. Y. W. Lee, B. Y. Kim, K. H. Lee, W. J. Song, G. Cao, K. W. Park, *Int. J. Electrochem. Sci.*, 8 (2013) 2305.
22. C. Xu, Y. Hu, J. Rong, S. Jiang, Y. Liu, *Electrochem. Commun.*, 9 (2007) 2009.
23. Q. F. Yi, W. Huang, W. Q. Yu, L. Li, X. P. Liu, *Chin. J. Chem.*, 26 (2008) 1367.
24. C. Xu, J. Hou, X. Pang, X. Li, M. Zhu, B. Tang, *Int. J. Hydrogen Energy*, 37 (2012) 10489.
25. S. Yan, L. Gao, S. Zhang, L. Gao, W. Zhang, Y. Li, *Int. J. Hydrogen Energy*, 38 (2013) 12838.
26. L. Lu, S. Zhang, S. Yan, *Chinese Journal of Power Sources*, 38 (2014) 272.
27. P. Li, G. Guan, Q. Zhang, W. Zhao, R. Yuan, *Mater. Sci. Tech-Lond*, 9 (2001) 259.
28. N. Tateishi, K. Nishimura, K. Yahikozawa, M. Nakagawa, M. Yamada, Y. Takasu, *J. Electroanal. Chem.*, 352 (1993) 243.
29. K. Yahikozawa, K. Nishimura, M. Kumazawa, N. Tateishi, Y. Takasu, K. Yasuda, Y. Matsuda, *Electrochim. Acta*, 37 (1992) 453.
30. S. Yan, S. Zhang, Y. Lin, G. Liu, *J. Phys. Chem. C*, 115 (2011) 6986.
31. S. Yan, S. Zhang, *Int. J. Hydrogen Energy*, 37 (2012) 9636.
32. S. Yan, L. Gao, S. Zhang, W. Zhang, Y. Li, L. Gao, *Electrochim. Acta*, 94 (2013) 159.
33. T. Yang, L. Zhang, X. Li, D. Xia, *J. Alloy Compd.*, 492 (2010) 83.
34. V. Radmilovic, H. A. Gasteiger, P. N. Ross, *J. Catal.*, 154 (1995) 98.
35. S. Yan, S. Zhang, *Int. J. Hydrogen Energy*, 36 (2011) 13392.

© 2015 The Authors. Published by ESG (www.electrochemsci.org). This article is an open access article distributed under the terms and conditions of the Creative Commons Attribution license (<http://creativecommons.org/licenses/by/4.0/>).